



Brazilian Journal of Physics

ISSN: 0103-9733

luizno.bjp@gmail.com

Sociedade Brasileira de Física
Brasil

Okumus, Mustafa; Özgan, Sükrü; Ylmaz, Süleyman
Thermal and Optical Properties of Some Hydrogen-Bonded Liquid Crystal Mixtures
Brazilian Journal of Physics, vol. 44, núm. 4, 2014, pp. 326-333
Sociedade Brasileira de Física
São Paulo, Brasil

Available in: <http://www.redalyc.org/articulo.oa?id=46431147004>

- How to cite
- Complete issue
- More information about this article
- Journal's homepage in redalyc.org

redalyc.org

Scientific Information System
Network of Scientific Journals from Latin America, the Caribbean, Spain and Portugal
Non-profit academic project, developed under the open access initiative

Thermal and Optical Properties of Some Hydrogen-Bonded Liquid Crystal Mixtures

Mustafa Okumuş · Şükrü Özgan · Süleyman Yılmaz

Received: 21 October 2013 / Published online: 21 May 2014
© Sociedade Brasileira de Física 2014

Abstract Phase transition properties of the mixtures of hydrogen-bonded nematic liquid crystals (HBLC) 4-hexylbenzoic acid (6BA), 4-(octyloxy)benzoic acid (8OBA), and 4-(decyloxy)benzoic acid (10OBA) have been investigated by means of differential scanning calorimetry (DSC) and polarize optic microscope (POM). The DSC and POM results clearly indicate the existence of smectic and nematic phase transitions in binary mixtures. The phase transition temperature values of 6BA/10OBA mixtures have clearly increased with increasing heating rate. The activation energies were calculated for the phase transitions of 6BA/10OBA liquid crystal (LC) mixture. The optical transmittance of these mixed hydrogen-bonded nematic liquid crystals was investigated in terms of temperature variations through electrooptic methods. The electrooptic experiments indicate that, while low in the nematic phase, the optical transmittance is very high at the nematic-isotropic phase transition. The transmitted light intensity values of 6BA/8OBA mixture are somewhat higher than those of other binary mixtures, 6BA/10OBA and 8OBA/10OBA, a result associated with the different alkyloxy chain lengths.

Keywords Liquid crystal mixtures · Thermodynamic properties · Optical properties

M. Okumuş (✉)
Metallurgical and Materials Engineering, Batman University,
Batman, Turkey
e-mail: mustafa.okumus@batman.edu.tr

Ş. Özgan
Department of Physics, Kahramanmaraş Sutcu Imam University,
46100 Kahramanmaraş, Turkey

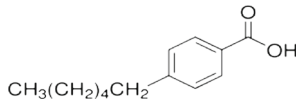
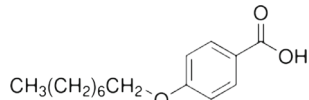
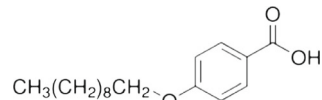
S. Yılmaz
Faculty of Education, Department of Elementary Education, Aksaray
University, Aksaray, Turkey

1 Introduction

Liquid crystals (LCs) are materials to be liquify in unique configurations in certain temperature (T) ranges and have both conventional liquid and solid crystal properties [1, 2]. The existence of liquid crystals has been known for more than a century, but in recent years, liquid crystal mixtures have become important as novel materials for display applications ranging from flat panel displays to laser beam steering and optical switching [3–7]. This is because they offer a number of potential advantages over the well-established nematic devices as well as over a number of other competitors. Several of liquid crystals in current display applications are eutectic mixtures of two or more mesogenic substances. Hydrogen-bonded liquid crystals (HBLC) and their complexes formed by mixtures have interesting properties, due to the intermolecular hydrogen bonds [8]. Hydrogen bonds enable various mesogenic and non-mesogenic compounds to form complexes which exhibit rich phase polymorphism. Typical representations of the liquid crystal substances constituted by hydrogen bonds in dimer molecules are 4,*n*-alkylbenzoic acids (nBA) and 4,*n*-alkyloxybenzoic acids (nOBA), where *n* is the number of carbons in the *n*-alkyl tails. HBLC materials are known since early 1960s [9]. Although many studies have been carried out on these pure liquid crystals in the last two decades [10–15], there is not enough study on their mixtures.

As it is well known, nematic liquid crystal mixtures are commonly used in optical processing systems and photonic devices. Phase transition behaviors, optical properties, and electrooptic effects provide the basis for liquid crystal display technology. Therefore, this treatise of the thermo-optical properties of nematic liquid crystal mixtures has substantial significance in technological applications [16]. The investigation of thermo-optical properties of nematic liquid crystal mixtures, which have single optical axis and stable structure, will considerably benefit from the determination of the physical properties

Fig. 1 Chemical structures of 4-hexylbenzoic acid, 4-(octyloxy)benzoic acid, and 4-(decyloxy)benzoic acid

LC	Chemical Structure	Linear Formula
6BA		$\text{CH}_3(\text{CH}_2)_5\text{C}_6\text{H}_4\text{CO}_2\text{H}$
8OBA		$\text{CH}_3(\text{CH}_2)_7\text{OC}_6\text{H}_4\text{CO}_2\text{H}$
10OBA		$\text{CH}_3(\text{CH}_2)_9\text{OC}_6\text{H}_4\text{CO}_2\text{H}$

of these materials [17]. This considered, we here target the development of liquid crystal mixtures. In order to design these processes, it is important to have a detailed knowledge of optical, electrical, electro-optical, and thermal properties of the nematic liquid crystal mixtures. In this study, we present experimental results on thermo-electro-optic properties for binary mixtures of 4-hexylbenzoic acid (6BA), 4-(octyloxy)benzoic acid (8OBA), and 4-(decyloxy)benzoic acid (10OBA), which show mesomorphic behavior because of the presence of a sufficiently high concentration of dimers, formed with hydrogen bonds. The 6BA, 8OBA, and 10OBA are the best known hydrogen-bonded liquid crystalline substances [18–22]. The 6BA, 8OBA, and 10OBA, as well as other members of the homologous series, are important for technological applications due to the possession of a good chemical stability.

2 Experimental

2.1 Materials

The hydrogen-bonded liquid crystal materials 4-hexylbenzoic acid (6BA), 4-(octyloxy)benzoic acid (8OBA), and 4-(decyloxy)benzoic acid (10OBA) were purchased from

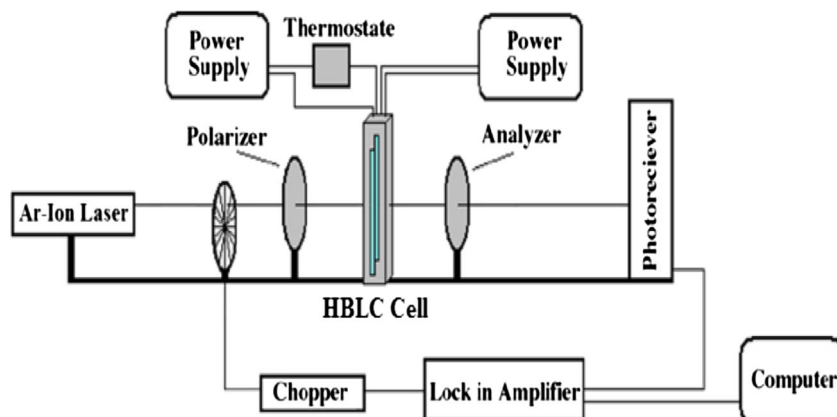
Sigma–Aldrich Corporation and were used without further purification, because their phase transition temperatures were in substantial agreement with the data given in the Sigma–Aldrich catalogue. The structure formula of 6BA, 8OBA, and 10OBA nematic hydrogen-bonded liquid crystals used in this study is shown in Fig. 1.

2.2 Thermal Analysis

The thermal properties of liquid crystals and their mixtures were investigated by a Perkin–Elmer differential scanning calorimeter (DSC–7) using continuous heating and cooling. Before use, the DSC was calibrated with indium (99.999 wt% pure In). Calibration is accomplished by running a standard material and comparing the experimental reliable temperature (melting point, clearing point) and enthalpy of transition to standard values. The experiments were carried out with scanning rates of 5, 10, 15, and 20 °C/min by means of DSC unit equipped with a data acquisition and analysis station.

The liquid crystal mixture samples were subject to heat treatment on the magnetic stirrer after they were mixed at room temperature. The heated samples were mixed with an injector needle before and after every phase transformation. The process was repeated carefully twice about every 40 min.

Fig. 2 Schematic representation of the heating and the optical measurement units



After that, DSC samples were prepared in a thin aluminum pan, which was then placed on the stage of a piston-like sample crimper. The DSC was initially cooled to 10 °C, and each sample was left in the pan for 2 min to ensure that thermal equilibrium was reached. Then the temperature was run at different heating rates from 10 to 160 °C, which is above the reported clearing point [23–26], and held at 160 °C for 2 min to ensure complete transformation to the isotropic phase. After that, DSC was cooled at different cooling rates from 160 to 10 °C.

2.3 Optical Analysis

The pure hydrogen-bonded liquid crystals and their mixtures were used in the liquid-crystal sandwich-cell preparation. The liquid crystal cells were formed by two glass plates with a spacer with thickness of 50 μm between them. Firstly, the two glass plates were cleaned carefully by using acetone and alcohol and then washed by deionized and bidistilled water in an ultrasonic combat bath. Sandwiching the LC sample between the pretreated substrates of the cell ensures homogeneous alignment. The pure LC and mixed material were placed into the cell in its high-temperature isotropic state by the capillary action method. The phase transition properties were investigated based on the textural changes that were observed during heating or cooling cycles of the sample. All binary mixture samples were prepared at the rate of 1:1 (in wt%). Morphologic structure and phase transition temperatures in all HBLC samples were investigated by using a Leica 180 DM LP polarization microscope with a thermal table and a CCD camera. A thin sample sandwiched between two glass cover slips was placed inside the thermal table, and the temperature was raised to 150 °C at the rate of 30 °C/min and kept at that temperature for 5 min to ensure complete isotropic. Then the sample was cooled to 20 °C at a rate of 10 °C/min, and then kept at different

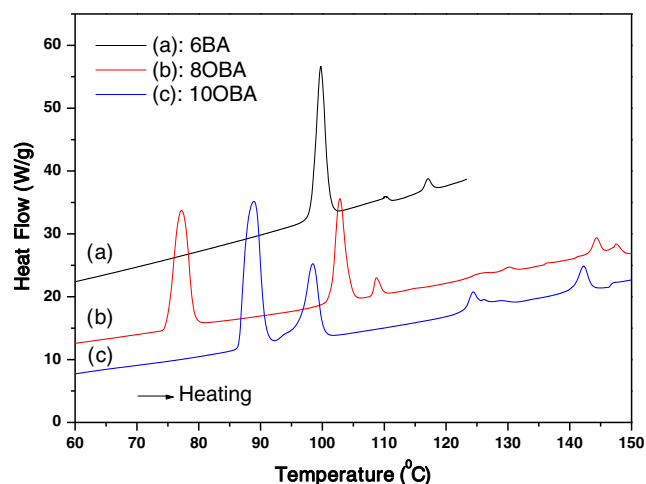


Fig. 3 DSC curves obtained during continuous heating of liquid crystals, 6BA, 8OBA, and 10OBA

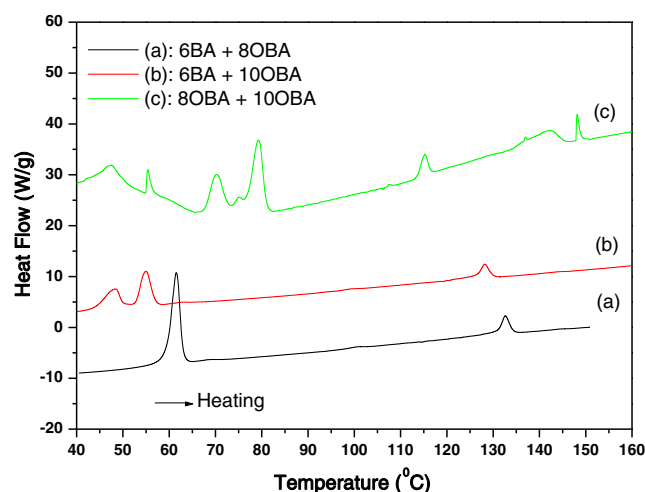


Fig. 4 DSC curves obtained during continuous heating of liquid crystal mixtures

temperatures for spherulite growth observation. As seen in Fig. 2, the optical transmitted light intensity measurement system consists of Lasos Ar-Ion laser with 514.5 nm, photoreceiver, SR530 Lock in Amplifier, SR540 optical chopper, and our own designed sample holder providing heating and optical apparatus such as polarizer and analyzer. The regular increments of the temperature were provided by the temperature control unit to include all of the phases for the HBLC samples. The experimental data obtained by the transmitted light intensity measurement system were transferred to a computer via RS-232 serial interface and compiled with the LabVIEW 8 program.

3 Results and Discussion

Recent investigations have shown that the 4-*n*-alkylbenzoic acids and 4-*n*-alkoxybenzoic acids have interesting structural and physical properties. In liquid crystals, similar ones are

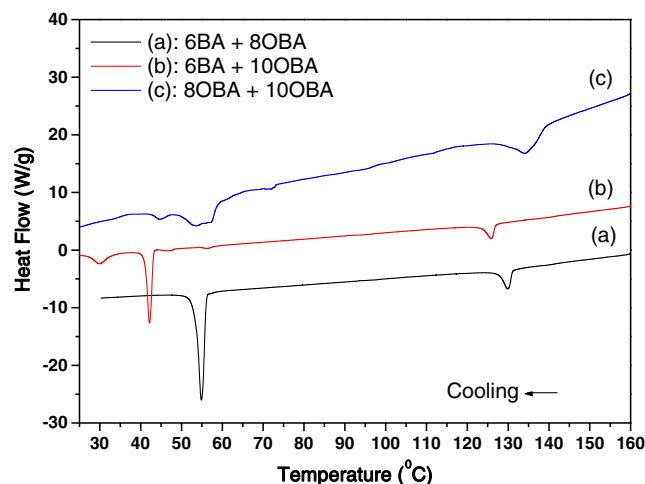


Fig. 5 DSC curves obtained during continuous cooling of liquid crystal mixtures

Table 1 The phase transition peak temperatures (T) and enthalpies (ΔH) of the pure liquid crystals and their mixtures

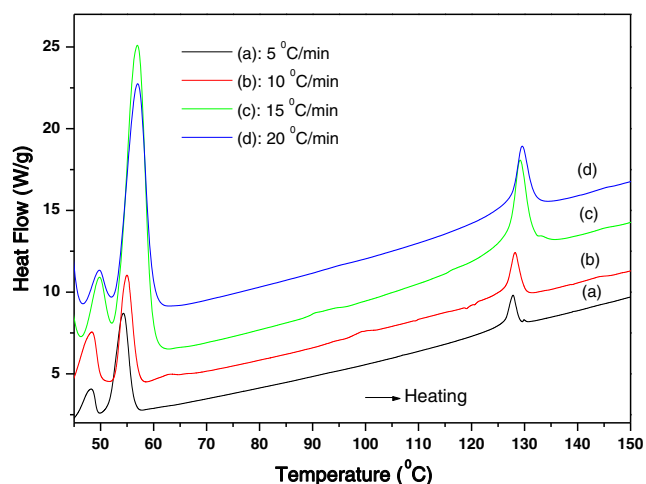
LC mixture	T_{CrA} (°C)	ΔH_{CrA} (J/g)	T_{CrN} (°C)	ΔH_{CrN} (J/g)	T_{AN} (°C)	ΔH_{AN} (J/g)	T_{AC} (°C)	ΔH_{AC} (J/g)	T_{CN} (°C)	ΔH_{CN} (J/g)	T_{NI} (°C)	ΔH_{NI} (J/g)
6BA	—	—	99.7	258.2	—	—	—	—	—	—	117	11.6
8OBA	77.2	306.6	—	—	—	—	102.8	194.1	108.7	20.2	144.3	19.2
10OBA	88.9	389.5	—	—	—	—	98.4	160.5	124.3	24.7	142.2	49.1
6BA+8OBA	—	—	61.5	256.4	—	—	—	—	—	—	132.6	39.7
6BA+10OBA	48.2	79.2	—	—	54.9	99.6	—	—	—	—	128.2	30.7
8OBA+10OBA	70.2	116	—	—	—	—	79.3	177.6	115.2	45.9	148.8	22.2

mixed with each other, and the transition temperature varies with the mixing rate in accordance with the change in phase from crystal to liquid crystal. The largest nematic range, used in determining the quality of the liquid crystals, is the eutectic mixture point that is nearly the ratio of 50:50 wt%. In this study, we have examined the nematic range and phase identification of binary mixtures to assess the effect of the blends. Figure 3 shows the DSC heating curves of pure hydrogen-bonded liquid crystals 6BA, 8OBA, and 10OBA. As for pure 8OBA and 10OBA, the stable mesophase sequence on heating from room temperature is crystalline (Cr)–smectic A (SmA)–smectic C (SmC)–nematic (N)–isotropic (I), whereas for pure 6BA, the SmA and SmC mesophases are absent in the mesophase sequence: Cr–N–I. The liquid crystals were assessed to be highly pure, because they showed sharp transition temperatures in good agreement with those literatures [27–30].

The DSC curves for HBLC binary mixtures (at rate of 1:1) obtained by heating from the crystalline to isotropic phase with heating rate 10 °C/min are shown in Fig. 4. As seen in Fig. 4, the DSC curves of HBLC binary mixtures exhibit the different endothermic peaks, indicating that structural transformation into isotropic phase takes places in steps. These

binary mixtures consisted of several phases: crystal, smectic A, smectic C, nematic liquid crystal, and isotropic liquid. In the case of 6BA and 8OBA mixed at rate of 1:1, for example, transitions were observed from crystal to nematic liquid crystal at 61.52 °C and from nematic liquid crystal to liquid at 132.63 °C. The transition temperatures were determined from the values of temperatures corresponding to the peak of the DSC thermogram. The enthalpies (H) of the phase transitions were determined from the areas under the DSC peaks of the transitions. While the smectic phase was not observed in 6BA/8OBA mixture, it was observed in 6BA/10OBA and 8OBA/10OBA binary mixtures, and also, these observations were confirmed by the POM experiments. The smectic phase diversity increased with increasing alkyloxy chain length. If the alkyl chain does not exist in a binary mixture, such as 8OBA/10OBA mixture, the smectic phase diversity increases, and the nematic range of HBLC mixtures decreases. The largest nematic range occurred in the 6BA/10OBA mixture with a temperature range of 73.23 °C. According to the DSC results, the nematic ranges of HBLC mixed with 6BA in 8OBA and 10OBA are wider than the nematic range of 8OBA/10OBA mixture and the pure blends. The results indicate that alkyloxy chain of HBLC exhibits a rich diversity of liquid crystal behaviors including smectic phases, and that the 6BA/10OBA mixture is more convenient for applications.

The DSC curves for HBLC binary mixtures obtained by cooling from the isotropic to crystalline phase with cooling rate of 10 °C/min are shown in Fig. 5. It can be seen that the phase transition peak shapes observed by DSC cooling are very similar to the phase transition peak shapes observed in the heating process. However, the phase transition

**Fig. 6** DSC curves obtained during continuous heating of 50 % 6BA and 50 % 10OBA liquid crystal mixture at different heating rates**Table 2** Activation energies E_A (kJ/mol) for phase transitions of 50 % 6BA and 50 % 10OBA liquid crystal mixture

Activation energy	Crystal-smectic A	Smectic A-nematic	Nematic-isotropic
Ozawa (kJ/mol)	503±10	349±10	908±10
Kissenger (kJ/mol)	523±10	362±10	948±10
Takhor (kJ/mol)	528±10	368±10	955±10

Table 3 The phase transition peak temperatures (T) and enthalpies (ΔH) of 50 % 6BA and 50 % 10OBA liquid crystal mixture as a function of heating rates

Heating rate (°C/min)	T_{CrA} (°C)	ΔH_{CrA} (J/g)	T_{AN} (°C)	ΔH_{AN} (J/g)	T_{NI} (°C)	ΔH_{NI} (J/g)
5	48.1	51.1	54.3	199.4	127.8	29.9
10	48.2	79.2	54.9	99.6	128.2	30.7
15	49.7	24.6	56.9	207.8	129.1	33.3
20	49.7	17.8	57.0	213.5	129.5	32.3

temperatures on cooling curves are smaller than the of phase transition temperatures obtained by heating. Nonetheless, one can see that the heating and cooling curves are nearly symmetrical relative to the x-axis.

The results of the thermal analyses, the phase transition temperatures of crystalline–smectic A, T_{CrA} ; smectic A–smectic C, T_{AC} ; smectic C–nematic, T_{CN} ; crystalline–nematic, T_{CrN} ; smectic A–nematic, T_{AN} ; nematic–isotropic, T_{NI} ; and the enthalpies ΔH_{CrA} , ΔH_{CrN} , ΔH_{AC} , ΔH_{CN} , ΔH_{AN} , and ΔH_{NI} , of those phase transitions are presented in Table 1. As seen in Table 1, the phase transition temperatures and enthalpies obtained in our experiments are approximately similar to the values reported in literatures [22–24, 31].

The phase transition temperature is dependent on the heating rate. Figure 6 shows the dependence of phase transition temperature on the heating rate for the 50 % 6BA and 50 % 10OBA liquid crystal mixtures. The obtained values can be used to estimate the associated phase transition activation energy (E_A) by means of the Ozawa [32], Kissinger [33], and Takhor [34] methods. According to all of the three methods, the activation energy (E_A) changes with temperature, or in other words, the environment of the rotating molecule changes with temperature. So, the activation energy can help us to speculate about the energy attributable to a molecular rotational mode. The activation energies, calculated by using Ozawa, Kissinger, and Takhor methods, are presented in Table 2 for the phase transition peak temperatures T_{CrA} ,

T_{AN} , and T_{NI} of 50 % 6BA and 50 % 10OBA liquid crystal mixtures. As seen in Table 2, the calculated values of the overall activation energy for the nematic–isotropic phase transition are higher than those of the crystalline–smectic A and smectic A–nematic phase transitions, indicating a relatively nematic liquid crystal structure. Here again, good agreement exists among three methods. The higher activation energy implies that the energy barrier for the nematic–isotropic phase transformation is higher than the energy barrier for the smectic A–nematic phase transformation and that the nematic structure is more stable than the smectic A structure at temperatures lower than the isotropization temperature. Similar results were reported in the literature [35–37] for phase transition activation energy of liquid crystals.

The heating rate is an important parameter because it introduces a controllable time scale. In this study, as the heating rate increases from 5 to 20 °C/min, the phase transformations occur in a shorter time by decreasing from 26 to 6.7 min, respectively, because of more heat energy. As seen in Fig. 6 and Table 3, the peak phase transition temperatures grow as the heating rate rises from 5 to 20 °C/min. While the peak enthalpies are usually decreasing at crystalline to smectic A transitions, the peak enthalpies increase at the smectic A to nematic and nematic to isotropic transition as the heating rate increases from 5 to 20 °C/min. Sometimes, the peak enthalpies are smaller or bigger than the other values of enthalpy for the same phase transitions by increasing heating rate. For example, the enthalpy of the smectic A to nematic phase transition is 199.49 J/g at 5 °C/min heating rate, which may be influenced by the crystalline to smectic A transition at a small heating rate. The peak heights of smectic A to nematic transitions are much higher than those of the crystalline to smectic A and nematic to isotropic transitions. The correlation of the phase transition temperatures and peak heights to the heating rate was observed to be in line with the results reported in the literature [35–37]. One can find a detailed comparison between the trends observed in the present study and the tendencies identified in previous studies [35–38]. We

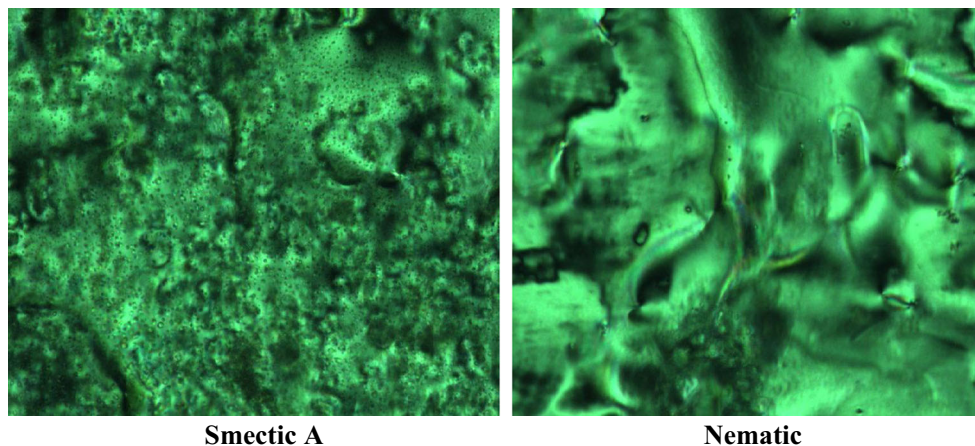
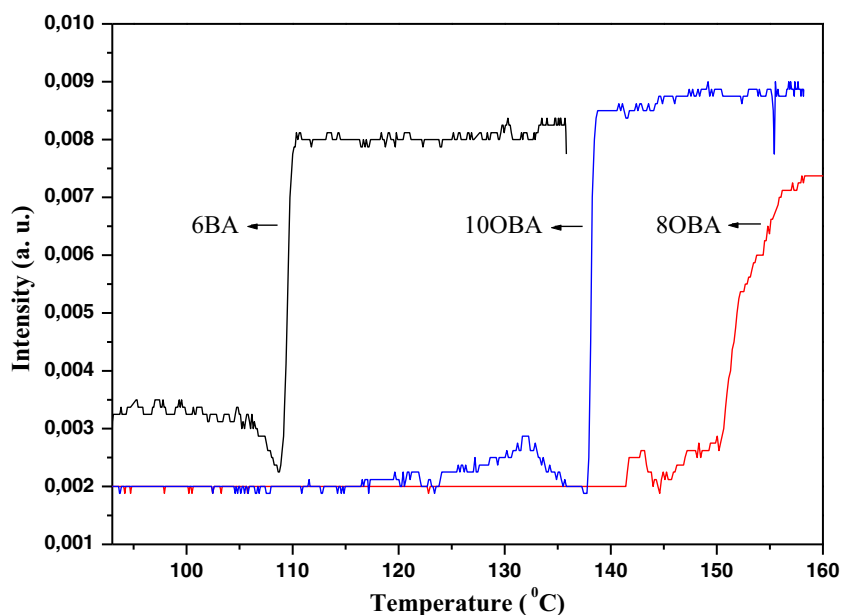
Fig. 7 Morphologic textures observed by POM of 50 % 6BA and 50 % 10OBA liquid crystal mixture on cooling; smectic A at 35.0°C, nematic at 90.0 °C

Fig. 8 The curves of transmitted intensity versus temperature of liquid crystals, 6BA, 8OBA, and 10OBA



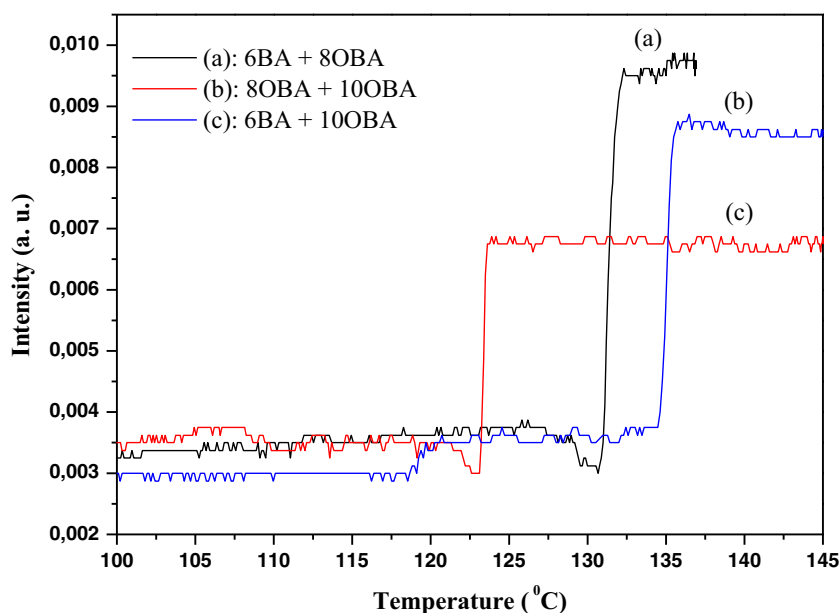
considered that the heating rate must be lower to observe a linear heating rate. The heating rate dependence of the peak shape of the liquid crystal mixture transitions is very complex.

Morphologic textures and phase transition temperatures of the 6BA, 8OBA, 10OBA, and their binary mixtures were carried out by means of POM. The morphologic properties are determined on the basis of the textural changes observed during the heating or cooling cycles of the LC sample. The morphologic textures of LC phases were identified by their comparison with the standard [39] textures. The observed textures from the POM experiments were presented in Fig. 7. As seen in Fig. 7, the phase textures of 6BA/10OBA were found to be smectic A and nematic during both heating

and cooling processes. On the other hand, smectic C phase was observed in pure 8OBA, 10OBA, and 8OBA/10OBA mixtures by POM at heating or cooling process. Smectic phase was not observed in 6BA/8OBA mixtures during heating or cooling. The identified morphologic textures were in good agreement with those reported in the literatures [23, 31, 39]. Moreover, the phase transition temperatures values observed during the POM experiments were in line with the phase transition temperatures obtained in the DSC experiments.

The phase transition temperatures and transmitted light intensities of 6BA, 8OBA, 10OBA, and their mixtures were determined during cooling from isotropic to crystal by using the different technique [16] illustrated in Fig. 2. The

Fig. 9 The curves of transmitted intensity versus temperature of liquid crystal mixtures



transmitted light intensities from the samples sandwiched between two glass cover slips were monitored as a function of temperature. The data for transmitted light intensity curves can be used to determine the phase transition temperatures. The curves of transmitted light intensity versus temperature for 6BA, 8OBA, and 10OBA are shown in Fig. 8. It is seen that the transmitted light intensity rises drastically at certain onset temperatures, which corresponds to phase transitions, as also confirmed by DSC and POM. As seen in Fig. 8, the transmitted light intensity from the samples increased clearly at the nematic to isotropic phase transition temperature, but it did not change much at the smectic to nematic phase transition temperature due to molecular anisotropy. While the transmitted light intensities of 8OBA and 10OBA in the nematic phase are approximately the same, the transmitted light intensity of 6BA in the nematic phase is higher. On the other hand, while the transmitted light intensity values of 6BA and 10OBA in the isotropic phase are approximately same, the transmitted light intensity value of 8OBA in the isotropic phase is smaller. Figure 9 shows the transmitted light intensity curves versus temperature of binary HBLC mixtures during cooling from isotropic to crystal. As seen in Fig. 9, the observed light intensity values increased suddenly during nematic-isotropic phase transition due to molecular anisotropy with alkyl or alkoxy chain length. The phase transition temperatures obtained from the data of Fig. 9 are in good agreement with the results of DSC experiments shown in Fig. 5, as also confirmed by POM. In addition, the transmitted light intensity values in the isotropic phase are higher than the transmitted light intensity values in the nematic phase, and also, the transmitted light intensity values of binary mixtures are higher than the transmitted light intensity values of pure HBLCs, 6BA, 8OBA, and 10OBA. Similar results for the behavior of transmitted light intensity were reported in the literature [16, 17, 40, 41].

4 Conclusions

The DSC curves that were used to determine the phase transition temperatures and enthalpies showed the existence of phase transitions in hydrogen-bonded liquid crystal mixtures of the 6BA/8OBA, 6BA/10OBA, and 8OBA/10OBA during continuous heating or cooling. The nematic range of the 6BA/10OBA mixture is the widest, with a 73.23 °C temperature range, among 6BA/8OBA, 8OBA/10OBA, and their pure blends. In this study, the activation energies of phase transitions in the 6BA/10OBA mixture were calculated for the first time by using Ozawa, Kissinger, and Takhor methods. The calculated activation energies showed good agreement among the three methods. The peak phase transition temperatures increased by increasing heating rate from 5 to 20 °C/min. While the peak enthalpies usually decrease at the crystalline to smectic A transition, the peak enthalpies increase at the

smectic A to nematic and nematic to isotropic transitions as the heating rate rises. The morphologic textures and phase transition temperatures of the binary mixtures, 6BA/8OBA, 6BA/10OBA, and 8OBA/10OBA were identified by POM observations. The transmitted light intensities obtained from the HBLC samples were monitored as a function of temperature. The results show that the transmitted light intensities increase in the isotropic phase and decrease in nematic phase due to the molecular anisotropy with alkyl or alkoxy chain length. The transmitted light intensity values of binary mixtures are higher than the transmitted light intensity values of pure HBLCs.

Acknowledgments The work has been supported by Kahramanmaraş Sutcu Imam University Scientific Research Projects Coordination Department under Project Number: 2011/3-43 D.

References

1. E.B. Priestley, P.J. Wojtowicz, P. Sheng, *Introduction to liquid crystals* (Plenum Press, London, 1974)
2. D. Demus, J. Goodby, G.W. Gray, H.W. Spiess, V. Vill, *Handbook of Liquid Crystals*, vols. 1–3, (Wiley–VCH, 1998)
3. J.W. Doane, *Liquid crystals—applications and uses*. World Sci. Singap. **1**, 361–395 (1990). Edited B. Bahadur
4. H.S. Kitzerow, *Liq. Cryst.* **16**, 1 (1994)
5. K. Ichimura, *Chem. Rev.* **100**, 1847 (2000)
6. S. Chandrasekhar, *Liquid crystals*, 2nd edn. (University Press, Cambridge, 1992)
7. P.G. De Gennes, J. Prost, *The physics of liquid crystals*, 2nd edn. (Oxford Science Publications, Clarendon Press, Oxford, 1993)
8. B. Katranchev, H. Naradikian, M. Petrov, *J. Optoelectron. Adv. Mater.* **7**, 273 (2005)
9. G.W. Gray, *Molecular structure and properties of liquid crystals* (Academic, London, 1962)
10. T. Kato, J.M.J. Frechet, *J. Am. Chem. Soc.* **111**, 8533 (1989)
11. J.W. Goodby, R. Blinc, N.A. Clark, S.T. Lagerwall, S.A. Osipov, S.A. Pikin, T. Sakurai, Y. Yoshino, B. Zecks, *Ferro electric liquid crystal, principles properties and applications* (Gorden and Breach Press, Philadelphia, 1991)
12. S. Malik, P.K. Dhal, R.A. Mashelkar, *Macromolecules* **28**, 2159 (1995)
13. P.A. Kumar, M. Srinivasulu, V.G.K.M. Pisipati, *Liq. Cryst.* **26**, 859 (1999)
14. M. Srinivasulu, P.V.V. Satyanarayana, P.A. Kumar, V.G.K.M. Pisipati, *Liq. Cryst.* **28**, 1321 (2001)
15. P. Swathi, S. Sreehari Sastry, P.A. Kumar, V.G.K.M. Pisipati, *Mol. Cryst. Liq. Cryst.* **365**, 523 (2001)
16. S. Yilmaz, *Mater. Chem. Phys.* **110**, 140 (2008)
17. S. Yilmaz, A. Bozkurt, *Mater. Chem. Phys.* **107**, 410 (2008)
18. V.N. Vijayakumar, K. Murugadass, M.L.N. Madhu Mohan, *Mol. Cryst. Liq. Cryst.* **515**, 39 (2009)
19. V.N. Vijayakumar, M.L.N. Madhu Mohan, *J. Mol. Struct.* **1000**, 69 (2011)
20. V.N. Vijayakumar, M.L.N. Madhu Mohan, *J. Mol. Struct.* **991**, 60 (2011)
21. N. Pongali Sathya Prabu, V.N. Vijayakumar, M.L.N. Madhu Mohan, *Physica B* **406**, 1106 (2011)
22. V.N. Vijayakumar, M.L.N. Madhu Mohan, *Physica B* **406**, 4139 (2011)

23. L. Guang Chen, *Thermo-Optical Properties of Polymer Dispersed Liquid Crystals*, Ph.D. Thesis, (RMIT University, 2007)
24. V.N. Vijayakumar, M.L.N. Madhu Mohan, Solid State Commun. **149**, 2090 (2009)
25. B. Katranchev, M. Petrov, Bulg. J. Phys. **31**, 111 (2004)
26. M. Petrov, P. Simova, Liq. Cryst. **7**, 203 (1990)
27. V.P. Privalko, G.A. Puchkovskaya, E.N. Shermatov, A.A. Yakubov, Mol. Cryst. Liq. Cryst. **126**, 289 (1985)
28. M.J.S. Monte, A.R.R.P. Almeida, M.A.V. Riberio da Silva, J. Chem. Thermodyn. **36**, 385 (2004)
29. D. Demus, H. Demus, H. Zschke, *Flüssige Kristalle in Tabellen* (Deutscher Verlag für Grundstoffindustrie, Leipzig, 1974)
30. T. Kato, J.M.J. Frechet, P.G. Wilson et al., Chem. Mater. **5**, 1094 (1993)
31. M. Muniprasad, M. Srinivasulu, P.V. Chalapathi, D.M. Potukuchi, J. Mol. Struct. **1015**, 181 (2012)
32. T. Ozawa, J. Therm. Anal. **2**, 301 (1970)
33. H.E. Kissinger, Anal. Chem. **29**, 1702 (1957)
34. R.L. Takhor, *Advances in nucléation and crystallization of glasses* (Americal Chemical Society, Columbus, 1971), pp. 166–172
35. Y.H. Gursel, B.F. Senkal, M. Kandaz, F. Yakuphanoglu, Polym. Adv. Technol. **22**, 90 (2011)
36. L. Minhui, W. Xiaogong, L. Deshan, Z. Qixiang, Chin. J. Polym. Sci. **9**, 14 (1991)
37. Ş. Özgün, M. Okumuş, Braz. J. Phys. **41**, 118 (2011)
38. M. Okumuş, S. Özgün, Asian J. Chem. **25**, 3879 (2013)
39. G.W. Gray, J.W. Goodby, *Smectic liquid crystals—textures and structures* (Leonard Hill, London, 1984)
40. H. Özbek, S. Yıldız, Ö. Pekcan, Y. Hepuzer, Y. Yağcı, G. Galli, Mater. Chem. Phys. **78**, 318 (2002)
41. R.R. Deshmukh, M.K. Malik, J. Appl. Polym. Sci. **108**, 3063 (2008)